Design, synthesis, and evaluation of 8-aminoquinoline-melatonin derivatives as effective multifunctional agents for Alzheimer's disease

Ziwei Chen[1], Xuefeng Yu[1], Lei Chen[1], Lexing Xu[1], Yu Cai[1], Shanshan Hou[1], Miaodan Zheng[2], Fuhe Liu[1]

[1]Pharmaceutical Department, Zhejiang Pharmaceutical College, Ningbo, China; [2]Pharmacy Department, Ningbo Medical Center Lihuili Hospital, Ningbo, China

Contributions: (I) Conception and design: F Liu; (II) Administrative support: F Liu; (III) Provision of study materials or patients: F Liu; (IV) Collection and assembly of data: Z Chen; (V) Data analysis and interpretation: Z Chen; (VI) Manuscript writing: All authors; (VII) Final approval of manuscript: All authors.

Correspondence to: Professor Fuhe Liu. Zhejiang Pharmaceutical College, Ningbo, China. Email: 710581327@qq.com.

Background: Alzheimer's disease (AD) is thought to be a complex, multifactorial syndrome with many related molecular lesions contributing to its pathogenesis. Thus, multi-target-directed ligands are considered an effective way of treating AD. This study sought to evaluate 8-aminoquinoline-melatonin derivatives as effective multifunctional agents for AD.

Methods: Thioflavin-T fluorescence assays were used to detect the inhibitory potency of 8-aminoquinoline-melatonin hybrids (a1–a5, b1–b5, and c1–c5) on self- and acetylcholinesterase (AChE)-induced amyloid-β (Aβ) aggregation. The AChE and butyrylcholinesterase (BuChE) inhibitory potency within the compounds was evaluated by Ellman's assays. Methyl thiazolyl tetrazolium (MTT) assays were performed to evaluate the cytotoxicity of the compounds to C17.2 cells. MTT assay was used to detect the cell viability of HT22 cells to evaluate the antioxidant effect of the compounds. Metal chelation property was measured by ultraviolet-visible spectrophotometry.

Results: Compounds c3 and c5 had superior inhibitory activity against self-induced Aβ aggregation (with inhibitory rates of 41.4±2.1 and 25.5±3.2 at 10 μM, respectively) compared to the other compounds. Compounds in the carbamate group (i.e., a4, a5, b4, b5, c4, and c5) showed significant BuChE inhibitory activity and excellent selectivity over AChE. Most of the compounds exhibited low cytotoxicity in the C17.2 cells. Notably, a2, a3, b2, and b3 and series c (c1–c5) exhibited strong protective effects. Additionally, a3 and c1 specifically chelated with copper ions.

Conclusions: Taking all of the promising results together, 8-aminoquinoline-melatonin hybrids can serve as lead molecules in the further development of new multi-functional anti-AD agents.

Keywords: Aminoquinoline; melatonin; Alzheimer's disease (AD); multifunctional agents

Introduction

Alzheimer's disease (AD) is characterized by progressive memory loss, language skill decline, and other cognitive impairments, and is a complex neurodegenerative disease with a multifaceted path mechanism. Studies show that AD is a frequently occurring disease in the elderly, and AD

has a great effect on the quality of life of patients and their families (1-3). Many countries have aging societies, which will place an enormous pressure on these societies. Thus, finding an effective drug for AD therapy has become an important research topic.

There is strong evidence that amyloid plaques (APs),
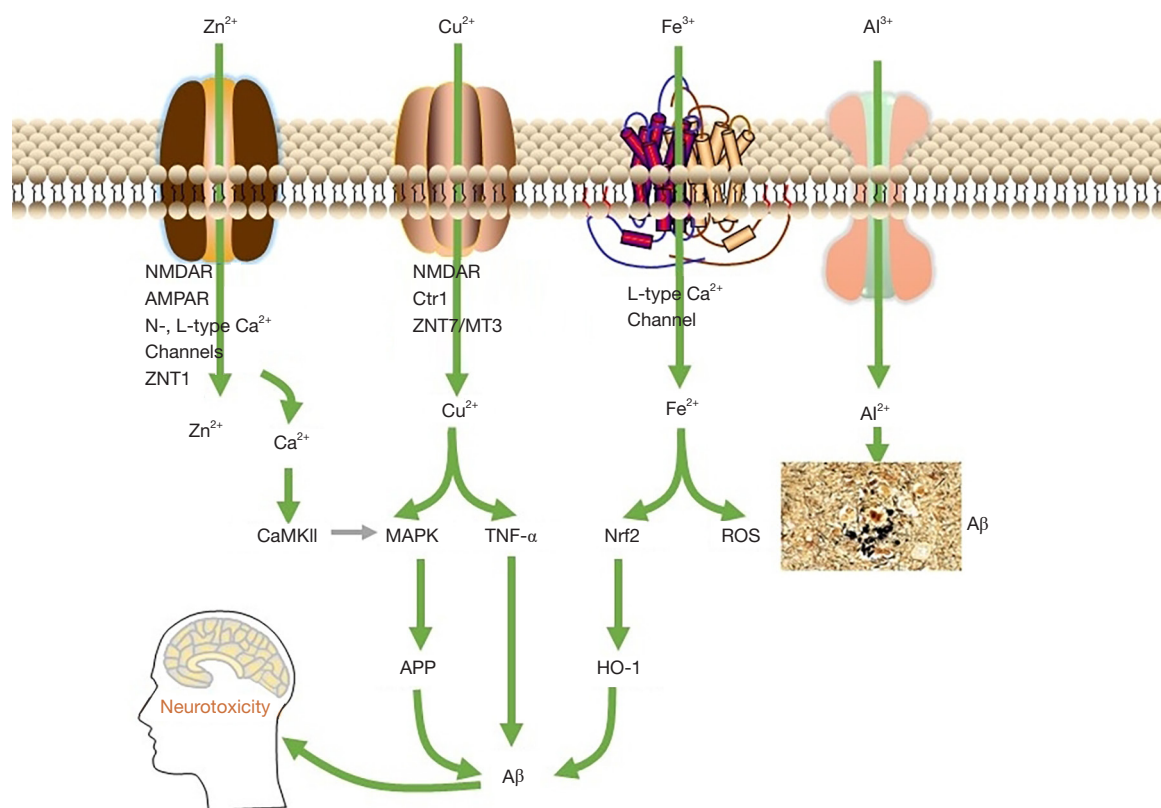
Figure 1 Relationship between AD and the homeostasis of metal ions. Aβ, amyloid-β; AD, Alzheimer's disease.

which are mainly composed of aggregated amyloid-β (Aβ) peptide, and neurofibrillary tangles (NFTs), which are composed of hyperphosphorylated tau protein, are the two most characteristic pathologic hallmarks of AD. Under the Aβ hypothesis, the accumulation of aberrant, misfolded Aβ peptide in the central nervous system (CNS) is well recognized and accepted (4,5). In the past 20 years, different laboratories have designed disease-modifying therapies that aim to prevent Aβ production or increase its degradation. However, new drug discovery strategies have had to be reconsidered, as approximately 100 AD drugs developed under this strategy failed from 1998 to 2011 (6). In fact, there is increasing evidence that APs and NFTs are not the only pathological mechanisms involved in the onset and progression of AD. Indeed, many other alterations, such as aggregation of Aβ, cholinergic and free radical damage, mental dyshomeostasis and neuron loss, are emerging as key features of AD (7,8).

Over the past two decades, a growing body of evidence has indicated that one of the potentially modifiable risk factors for dementia is the age-related imbalance of metal homeostasis. Research showed that the brain of AD patients is the presence of large amounts of metal ions [393 μmol/L of copper (Cu), 1,055 μmol/L of zinc (Zn), and 940 μmol/L of iron (Fe)], which are 3–6 times greater than those of a normal brain (9). High levels of metal ions, readily bind to Aβ and facilitate Aβ aggregation. Additionally, the interaction between redox-active metal ions and Aβ was demonstrated to generate reactive oxygen species, which lead to oxidative stress (OS) and, eventually, neuronal death in AD patients (see *Figure 1*) (10,11). Accordingly, metal-ion chelators are considered a promising tool for the treatment of AD.

Clioquinol (PBT-1) is the first anti-AD metal ion chelator to enter clinical trials and it is one of the few drugs with the efficacy of postponing the AD progression (12-14). PBT-1, as an ion carrier, improves the uptake of copper and zinc ions in nerve cells, thereby restoring AD-induced neuronal copper and zinc deficiency. PBT-2, as the second-generation drug of 8-hydroxyquinoline derivatives, was developed by the same company for curing AD. PBT-2 can effectively reduce $Aβ_{42}$ levels in cerebrospinal fluid (CSF) of AD animals. In the phase II clinical trials of PBT-
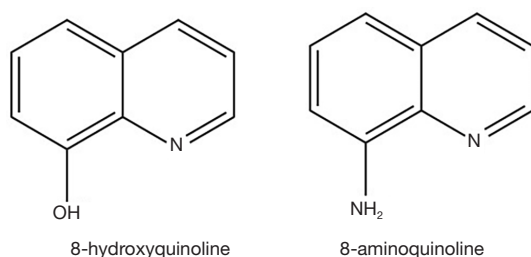
Figure 2 Selective metal-ion chelating agents for the pre-synthesis of the research group.

2, the drug is well tolerated and the level of $A\beta_{42}$ in CSF was reduced, and the patient's health condition was improved (15,16). The clinical trials of PBT-2 indicated that the development of metal ion modulator based on metal ion chelating agents is an acceptable and promising AD drug development strategy for AD therapy.

Research has shown that 8-hydroxyquinoline is a very important bidentate metal-ion chelating agent that forms a stable complex with a large number of transition metal ions (17). However, due to the universality of coordination, the lack of the necessary selectivity of the metal ions restricts its clinical application. Linker was introduced into the C2 position of 8-hydroxyquinoline to form new types of Bis-8-hydroxyquinoline (see *Figure 2*) that increase the chelating ability of Cu and Zn by 104–106 times. In vitro studies have shown that these novel chelating agents can effectively reverse the deposition of Cu and Zn ions induced by $A\beta$, and inhibit the formation of hydrogen peroxide induced by Cu^{2+}(18,19). Further, the selective coordination ability of 8-aminoquinoline with ions is better than that of 8-hydroxyquinoline, but 8-aminoquinoline only forms unstable metal complexes (20). Some new types of Bis-8-aminoquinoline have been reported to not only achieve the selective chelation of Cu ions (weakly complexed with Zn ions, which could not be detected), but also to greatly improve their chelating ability with Cu ions (max log K_{aff} value =17.9) (20).

Melatonin is a circadian rhythm–regulated and multifunctional molecule which plays a neuroprotective role against the pathogenesis of AD (21,22). Melatonin could directly scavenge free radicals and repair the damaged biomolecules, effectively protecting neurons and glial cells from $A\beta$-induced neurotoxicity and oxidative stress. It is reported that melatonin administration could reduce $A\beta$ accumulation and enhance cognitive function against neurodegenerative progression (23). Moreover, emerging

findings are revealing that the decreased melatonin production in aged person is considered as an important factor for developing AD (24,25). Thus, the significant neuroprotective effects of melatonin provide a novel strategy for the treatment of AD.

Cholinesterase inhibitors increase the availability of acetylcholine at synapses in the brain and are one of the few drug therapies that have been proven clinically useful in the treatment of Alzheimer's disease dementia, thus validating the cholinergic system as an important therapeutic target in the disease (26). AChE and BuChE are two different cholinesterase enzymes located in the brain that are responsible for acetylcholine hydrolysis. Initially, treatment efforts were focused on the inhibition of AChE; however, several studies have demonstrated the importance of both AChE and BuChE inhibition in the pathophysiology and pharmacological treatment of AD (27-30). Rivastigmine is a dual AChE–BuChE inhibitor, which has been approved in the US (FDA) for the treatment of mild, moderate, and severe AD (27).

Based on the above research, and according to the multi-target drug design ideas, we proposed to combine 8-aminoquinoline with melatonin and introduce effective pharmacophore of rivastigmine to produce a "multi-target, multi-functional" synergistic effect in the treatment of AD (see *Figure 3*). Our study describes the preparation and *in vitro* activities of novel 8-aminoquinoline-melatonin hybrids as inhibitors of AChE and BuChE, copper ion chelating agents and inhibitors of $A\beta$ aggregation. In addition, the toxicity as well as the neuroprotective activity against glutamate-induced cytotoxicity were also assessed. We present the following article in accordance with the MDAR reporting checklist (available at https://atm.amegroups.com/article/view/10.21037/atm-22-730/rc).

Methods

Pharmacological assays

In-vitro inhibition of AChE and BuChE

The inhibitory activity of the novel compounds a1–c5 against the cholinesterases was determined by the spectrophotometric method of Ellman et al, and absorbance was measured on a multidetection BioTek spectrophotometer. Acetylcholinesterase (AChE) was obtained from electric eels (EC 3.1.1.7), and butyrylcholinesterase (BuChE) from equine serum (EC 3.1.1.8). The AChE and BuChE solution was prepared by dissolving the lyophilized powder in phosphate

Page 4 of 19

Chen et al. Multifunctional agents for Alzheimer's disease
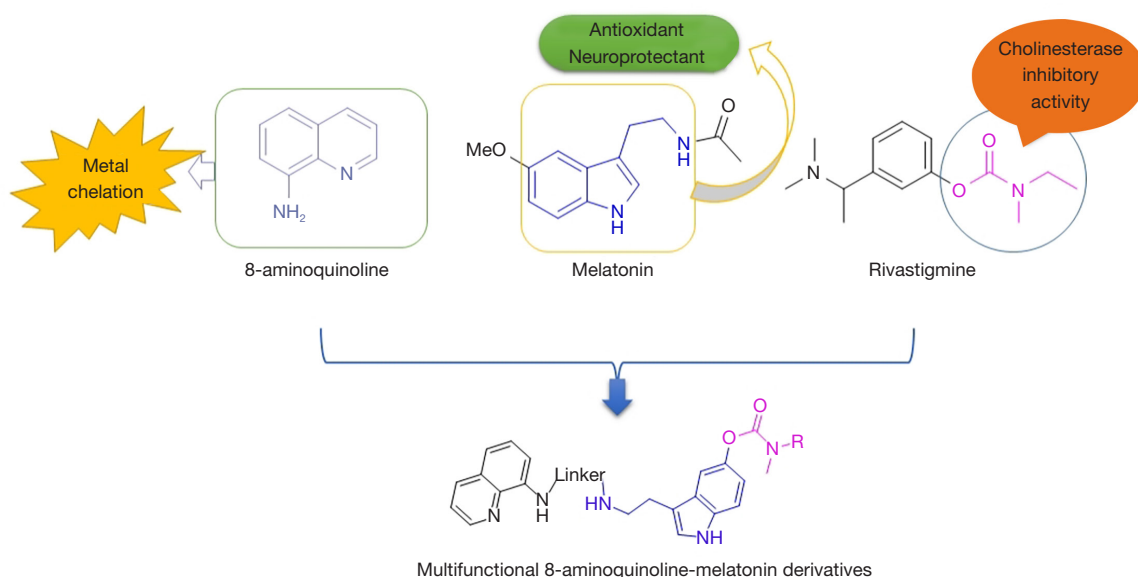
Figure 3 Design of multifunctional 8-aminoquinoline-melatonin hybrids.

buffer solution (PBS) (pH 8.0). Individual test compounds were dissolved in required volume of dimethylsulfoxide (DMSO) and diluted using PBS (pH 8.0) for the final range of concentrations. The assay solution (200 μL) consisted of PBS (pH 8.0) with 0.03 U/mL BuChE or 0.05 U/mL BuChE, 500 μM DTNB, different concentration of the compound (0.1, 0.5, 1, 5, 10, 20, 50 μM) and 500 μM of substrate [(Acetylthiocholine, ATC) or (Butylthiocholine, BTC)]. Test compounds were added to the assay solution and preincubated with the enzyme for 60 min, according to the kinetic type, followed by the addition of substrate. The same method was employed for the contrast using donepezil, melatonin or rivastigmine instead of a test compound. Blank assessments were performed with the reaction solutions in the absence of inhibitors following a similar method to afford 100% AChE or BuChE activity yields. The enzymatic reactions proceeded to completion in the plate within 5 min of incubation time at 37 ℃. Absorbance data of the mixtures were collected at 517 nm. Each concentration was analyzed in triplicate, and IC50 values were obtained by interpolation from the linear regression analysis and expressed as mean ± standard error of mean (SEM).

Cell cultures and treatments

C17.2 cell line from the European Collection of Cell Culture is mouse-derived multipotent neural stem cells isolated from the cerebellum and immortalized by the avian myelocytomatosis viral-related myc oncogene transfection.

HT22 cell line is a mouse immortalized hippocampal neuronal cell line without functional glutamate receptors. C17.2 (HTX2206C) and HT22 (HT-X1844) cell line were purchased from Shenzhen Haodi Huatuo Biotechnology Co., LTD. The HT22 cells were maintained in Dulbecco's Modified Eagle Medium (DMEM) supplemented with 10% (v/v) fetal bovine serum (FBS), and incubated at 37 ℃ under 5% carbon dioxide (CO_2). To study the protective effect of the test compounds on glutamate-induced neuronal death, the HT22 cells were seeded into 96-well plates. The cells in the control group were treated with the vehicle alone. The C17.2 cells were maintained in DMEM supplemented with 5% (v/v) FBS and 5% (v/v) horse serum, and then incubated at 37 ℃ under 5% CO_2. To study the toxicity of the test compounds on glutamate-induced neuronal death and their cell toxicity, the C17.2 cells were seeded into 96-well plates. The cells in the control group were treated with the vehicle alone.

ThT assays

The Thioflavin-T (ThT) fluorescence method was used to determine whether compounds restrained amyloid fibril formation. For the self-induced Aβ(1–40) aggregation: the assay solution (200 μL) consisted of 50 mM of glycine-NaOH buffer (pH 8.5) with 1.67 μM of ThT, 10 μM of $Aβ_{1-40}$ oligomers, 10 μM of test compounds or 0.215 M of PBS. Test compounds was incubated with $Aβ_{1-40}$ at 37 ℃ for 24 h, then 180 μL of ThT solution was added and

mixed, fluorescence was monitored with excitation at 446 nm and emission at 490 nm. The percentage inhibition of $A\beta_{1-40}$ aggregation due to the presence of test compounds was calculated using the following formula: $100 - (IFi/IF0 \times 100)$, where IF0 is the fluorescence intensities obtained for $A\beta_{1-40}$; IFi is the fluorescence intensities obtained for $A\beta_{1-40}$ plus the test compound.

For the AChE-induced Aβ(1–40) aggregation: the assay solution (200 μL) consisted of 50 mM of glycine-NaOH buffer (pH 8.5) with 1.67 μM of ThT, 230 μM of $A\beta_{1-40}$ oligomers, 2.3 μM of AChE, 100 μM of test compounds or 0.215 M of PBS.

Test compounds was incubated with $A\beta_{1-40}$ at 37 ℃ for 24 h, then 180 μL of ThT solution was added and mixed, fluorescence was monitored with excitation at 446 nm and emission at 490 nm. The percentage inhibition of $A\beta_{1-40}$ aggregation due to the presence of test compounds was calculated using the following formula: $100 - [(IFi - IF0')/(IF0 - IF0') \times 100]$, where IF0' is the fluorescence intensities obtained for $A\beta_{1-40}$; IF0 is the fluorescence intensities obtained for $A\beta_{1-40}$ plus AChE; IFi is the fluorescence intensities obtained for $A\beta_{1-40}$ plus AChE and test compound.

MTT assays

Cell viability was determined by Methyl thiazolyl tetrazolium (MTT) assays. The C17.2 cells (10,000 cells/well) were seeded into 96-well culture plates. After 24 h of incubation, the cells were further treated with different concentrations of test compounds (50, 100 μM). Cell growth was measured after 24 h. The HT22 cells (10,000 cells/well) were seeded into 96-well culture plates. After 24 h of incubation, the cells were further treated with different concentrations of test compounds (3, 10, 30 μM) for 30 min, and glutamate solution was then added (with a final concentration of 2 mM). Cell growth was measured after 24 h. MTT (10 μL, 5 mg/mL) was added to each well, and the mixture was incubated for 2 h at 37 ℃. The MTT reagent was then replaced with dimethyl sulfoxide (DMSO) (100 μL per well) to dissolve the formazan crystals. After the mixture was shaken at room temperature (RT) for 15 min, absorbance was determined at 570 nm using a microplate reader (Bio-Tek, USA). The results are expressed as the percentage of MTT reduction, and the absorbance of the control cells was set as 100%.

Metal-binding studies

The metal-binding studies were conducted using a Varioskan Flash Multimode Reader. The ultraviolet (UV)-vis spectra of a3 and c1 (50 μM) in the presence of 1 equiv (50 μM) of $CuCl_2$ (10 min incubation) or 20 equiv (1.0 mM) of other biological relevant metal ions (i.e., $ZnCl_2$, $MgCl_2$, $CaCl_2$, $MnCl_2$, $CoCl_2$, and $NiCl_2$, 30 min incubation) were recorded with wavelengths ranging from 200 to 600 nm.

Statistical analysis

All quantitative data and experiments described in this study were repeated at least three times. Differences between the groups were examined for multiple comparisons using a one-way analysis of variance with two-tailed unpaired Student's t-tests. All the data are expressed as the mean ± standard deviation. A P value <0.05 indicated a statistically significant difference.

Experimental section

Synthesis and characterization

Under this method 1H NMR spectra were recorded on Bruker Bio Spin GmbH at 400 and 100 MHz. The chemical shifts for 1H NMR and 13C NMR were referenced to TMS via residual solvent signals (CDCl3 at 7.26 and 77.0 ppm). Mass spectra (MS) were obtained using a Shimadzu LCMS-2010A instrument with an ESI or ACPI mass selective detector and high-resolution mass spectra (HRMS) on Shimadzu LCMS-IT-TOF. Melting points were uncorrected and recorded on an SRS-OptiMelt automated melting-point apparatus. Flash column chromatography was performed on silica gel (200–300 mesh). All the reagents were purchased from commercial suppliers, and were used without further purification.

Preparation of the 1-(2-(1H-indol-3-yl)ethyl)-3-(quinolin-8-yl) urea derivatives a1–a5

Under this method, 2,2,2-trichloroethyl carbonochloridate (1.26 g, 6.0 mmol) dropwise was added to a stirred solution of 8-amino-quinoline (0.71 g, 5.0 mmol) and i-Pr2NEt (1.29 g, 1.67 mL, 10.0 mmol) in THF at RT. The reaction mixture was stirred at RT for 4 h, and then quenched by the addition of water (10 mL). The reaction mixture was diluted with EtOAc (30 mL) and partitioned with water (20 mL). The organic fraction was washed with brine, dried over MgSO4, filtered and concentrated under reduced pressure to produce 2,2,2-trichloroethyl quinolin-8-ylcarbamate (1.52 g, 95%), a colorless oil, which was used in the next step without further purification.

1-(2-(1H-indol-3-yl) ethyl)-3-(quinolin-8-yl) urea (a1)

Under this method, 1, 8-diazabicyclo [5.4.0] undec-7-ene

Page 6 of 19

Chen et al. Multifunctional agents for Alzheimer's disease

(DBU, 0.46 g, 3.0 mmol) was added to a mixture of 2, 2, 2-trichloroethyl quinolin-8-ylcarbamate (0.64 g, 2.0 mmol) and tryptamine (0.32 g, 2.0 mmol) in MeCN (15 mL). The reaction mixture was heated at reflux for 3.5 hours, and then cooled, and the solvent was removed under reduced pressure. The residue was taken up in ethyl acetate and washed with water. The organic layer was separated and dried with MgSO4, filtered and concentrated. The resulting residue was purified by flash silica-gel column chromatography to afford the title compound (0.61 g, 92%) as a white solid. Melting points (mp) 159–162 ℃. 1H NMR (400 MHz, CDCl3) δ 8.92 (s, 1H), 8.69 (dd, J=4.2, 1.6 Hz, 1H), 8.56 (dd, J=7.7, 1.0 Hz, 1H), 8.12 (dd, J=8.3, 1.6 Hz, 1H), 8.08 (brs, 1H), 7.66 (d, J=7.8 Hz, 1H), 7.51 (t, J=8.0 Hz, 1H), 7.40–7.36 (m, 3H), 7.20 (dd, J=11.1, 4.0 Hz, 1H), 7.12 (t, J=7.2 Hz, 1H), 7.07 (d, J=2.2 Hz, 1H), 4.95 (t, J=5.5 Hz, 1H), 3.70 (dd, J=12.7, 6.6 Hz, 2H), 3.07 (t, J=6.7 Hz, 2H). 13C NMR (100 MHz, CDCl3) δ 155.1, 147.6, 138.2, 136.4, 136.4, 135.8, 128.1, 127.6, 127.3, 122.2, 122.2, 121.4, 119.5, 119.5, 118.8, 114.8, 113.1, 111.2, 40.6, and 25.9. HRMS ESI (+) m/z calculated for C20H19N4O [M+H] + 331.1559, found 331.1557.

1-(2-(5-methoxy-1H-indol-3-yl) ethyl)-3-(quinolin-8-yl) urea (a2)

Under this method, 1,8-diazabicyclo [5.4.0] undec-7-ene (DBU, 0.46 g, 3.0 mmol) was added to a mixture of 2,2,2-trichloroethyl quinolin-8-ylcarbamate (0.64 g, 2.0 mmol) and 5-methoxytryptamine (0.38 g, 2.0 mmol) in MeCN (15 mL). The reaction mixture was heated at reflux for 3.5 hours, and then cooled, and the solvent was removed under reduced pressure. The residue was taken up in ethyl acetate and washed with water. The organic layer was separated and dried with MgSO4, filtered and concentrated. The resulting residue was purified by flash silica-gel column chromatography to afford the title compound (0.61 g, 84%) as a white solid. Mp 188–191 ℃. 1H NMR (400 MHz, CDCl3) δ 8.90 (s, 1H), 8.69 (d, J=3.3 Hz, 1H), 8.55 (d, J=7.6 Hz, 1H), 8.12 (d, J=8.1 Hz, 1H), 7.99 (brs, 1H), 7.51 (t, J=8.0 Hz, 1H), 7.39 (dd, J=8.2, 3.7 Hz, 2H), 7.26 (t, J=4.2 Hz, 2H), 7.10–7.01 (m, 2H), 6.86 (dd, J=8.8, 2.2 Hz, 1H), 4.98 (brs, 1H), 3.80 (s, 3H), 3.69 (q, J=6.4 Hz, 2H), 3.04 (t, J=6.6 Hz, 2H). 13C NMR (100 MHz, CDCl3) δ 155.1, 154.2, 147.6, 138.1, 136.4, 135.8, 131.5, 128.1, 127.8, 127.6, 123.0, 121.4, 119.6, 114.8, 112.9, 112.6, 112.0, 100.5, 55.9, 40.7, and 25.9. HRMS ESI (+) m/z calculated for C21H21N4O2 [M+H] + 361.1665, found 361.1659.

1-(2-(5-hydroxy-1H-indol-3-yl) ethyl)-3-(quinolin-8-yl) urea (a3)

BBr3 (3 M in CH2Cl2, 2 mL) was added to a solution of 1-(2-(5-methoxy-1H-indol-3-yl) ethyl)-3-(quinolin-8-yl) urea (0.72 g, 2.0 mmol) in dry CH2Cl2 (10 mL) in an ice-water bath. The mixture was stirred overnight, and quenched with aqueous NaHCO3. The mixture was extracted with THF/EA (1:2, 20 mL×2). The combined organic layers were washed with brine and dried over MgSO4. The organic solvent was evaporated and the residue was purified by flash silica-gel column chromatography to afford the title compound (0.47 g, 68%) as a white solid. Mp 201–204 ℃. 1H NMR (400 MHz, CD3OD) δ 8.76 (dd, J=4.1, 1.4 Hz, 1H), 8.41 (d, J=7.5 Hz, 1H), 8.18 (dd, J=8.3, 1.3 Hz, 1H), 7.48–7.40 (m, 3H), 7.17 (d, J=8.6 Hz, 1H), 7.06 (s, 1H), 7.01 (d, J=2.1 Hz, 1H), 6.68 (dd, J=8.6, 2.2 Hz, 1H), 3.55 (t, J=7.3 Hz, 2H), 2.95 (t, J=7.3 Hz, 2H). 13C NMR (100 MHz, MeOD) δ 156.7, 149.7, 147.8, 138.3, 136.0, 135.9, 131.8, 128.2, 128.1, 126.8, 122.9, 121.3, 119.4, 114.3, 111.3, 111.2, 111.0, 102.2, 40.3, and 25.8. HRMS ESI (+) m/z calculated for C20H19N4O2 [M+H] + 347.1508, found 347.1504.

3-(2-(3-(quinolin-8-yl) ureido) ethyl)-1H-indol-5-yl dimethylcarbamate (a4)

Dimethylcarbamoyl chloride (151 mg, 129 μL, 1.4 mmol) followed by diisopropylethylamine (0.35 mL, 2.0 mmol) were added to a solution of 1-(2-(5-hydroxy-1H-indol-3-yl)ethyl)-3-(quinolin-8-yl)urea (0.35 g, 1.0 mmol) in dry pyridine (5 mL) at RT. The reaction mixture was heated to 70 ℃ and stirred overnight, then cooled, and the pyridine was removed under reduced pressure. The residue was taken up in CH2Cl2 and washed with water. The organic layer was separated and dried with MgSO4, filtered and concentrated. The resulting residue was purified by flash silica-gel column chromatography to afford the title compound (0.33 g, 80%) as white solid. Mp 110–113 ℃. 1H NMR (400 MHz, CDCl3) δ 9.02 (s, 1H), 8.73–8.63 (m, 2H), 8.59 (d, J=7.7 Hz, 1H), 8.09 (dd, J=8.3, 1.4 Hz, 1H), 7.48 (t, J=8.0 Hz, 1H), 7.41–7.32 (m, 2H), 7.26 (brs, 1H), 7.15 (d, J=8.7 Hz, 1H), 6.86 (dd, J=8.7, 2.1 Hz, 1H), 6.75 (d, J=1.7 Hz, 1H), 5.45 (brs, 1H), 3.38 (dd, J=12.6, 6.6 Hz, 2H), 3.12 (s, 3H), 3.02 (s, 3H), 2.70 (t, J=6.8 Hz, 2H). 13C NMR (100 MHz, CDCl3) δ 156.5, 155.6, 147.5, 144.6, 138.3, 136.3, 136.2, 134.1, 128.1, 127.6, 123.5, 121.3, 119.3, 116.3, 114.9, 112.9, 111.5, 111.1, 40.1, 36.8, 36.5, and 25.5. HRMS ESI (+) m/z calculated for C23H24N5O3 [M+H] + 418.1879, found 418.1875.

3-(2-(3-(quinolin-8-yl) ureido) ethyl)-1H-indol-5-yl ethyl (methyl) carbamate (a5)

N-ethyl-N-methylcarbamoyl chloride (169 mg, 1.4 mmol) followed by diisopropylethylamine (0.35 mL, 2.0 mmol)
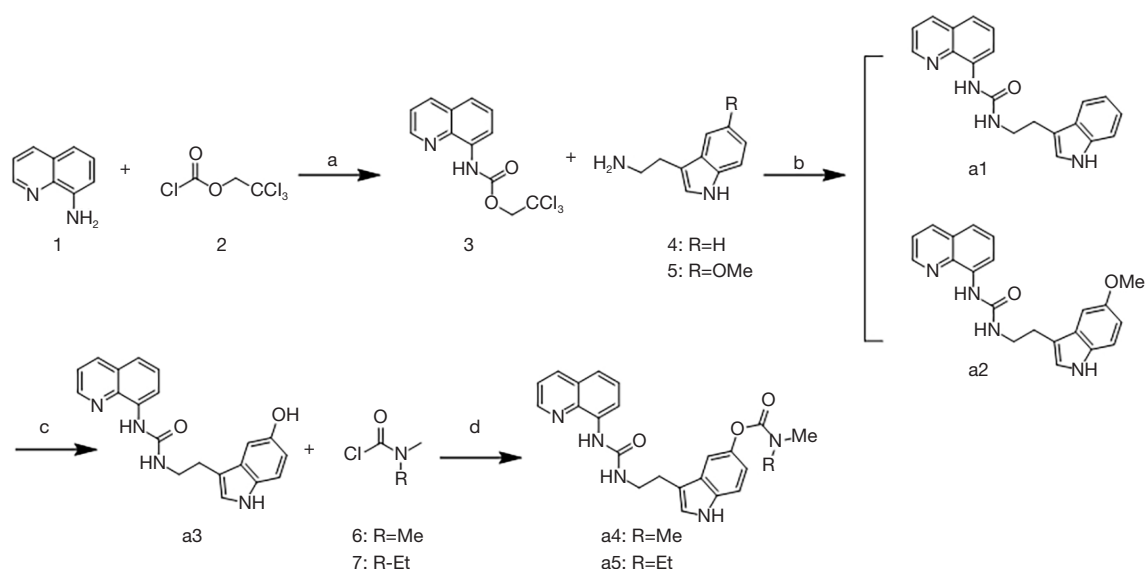
Figure 4 Synthesis of target compounds a1–a5. (a) i-Pr$_2$NEt, THF, RT; (b) DBU, MeCN, reflux, 3.5 h; (c) BBr$_3$, CH$_2$Cl$_2$, ice-bath; (d) i-Pr$_2$NEt, pyridine, 70 ℃.

were added to a solution of 1-(2-(5-hydroxy-1H-indol-3-yl)ethyl)-3-(quinolin-8-yl)urea (0.35 g, 1.0 mmol) in dry pyridine (5 mL) at RT. The reaction mixture was heated to 70 ℃ and stirred overnight, and then cooled, and the pyridine was removed under reduced pressure. The residue was taken up in CH2Cl2, and washed with water. The organic layer was separated and dried with MgSO4, filtered and concentrated. The resulting residue was purified by flash silica-gel column chromatography to afford the title compound (0.33 g, 77%) as white solid. Mp 112–115 ℃. 1H NMR (400 MHz, CDCl3) δ 9.00 (s, 1H), 8.68 (dd, J=4.2, 1.7 Hz, 1H), 8.66 (brs, 1H), 8.58 (dd, J=7.8, 1.2 Hz, 1H), 8.09 (dd, J=8.3, 1.7 Hz, 1H), 7.48 (t, J=8.0 Hz, 1H), 7.35 (ddd, J=8.3, 2.7, 1.4 Hz, 2H), 7.27 (d, J=8.3 Hz, 1H), 7.17 (dd, J=8.4, 3.7 Hz, 1H), 6.87 (d, J=8.7 Hz, 1H), 6.76 (d, J=2.1 Hz, 1H), 5.37 (brs, 1H), 3.5–3.42 (m, 2H), 3.39 (d, J=4.8 Hz, 2H), 3.05 (d, J=34.7 Hz, 3H), 2.71 (d, J=6.5 Hz, 2H), 1.31–1.11 (m, 3H). 13C NMR (100 MHz, CDCl3) δ 156.2, 155.6, 147.6, 144.6, 138.3, 136.3, 136.2, 134.1, 128.1, 127.6, 123.5, 121.3, 119.3, 116.3, 114.9, 112.9, 111.5, 111.1, 44.1, 40.1, 34.3, 33.8, 25.5, 13.3, and 12.6. HRMS ESI (+) m/z calculated for C24H26N5O3 [M+H] + 432.2036, found 432.2031.

Preparation of N-(2-(1H-indol-3-yl)ethyl)-2-(quinolin-8-ylamino)acetamidederivatives b1–b5

The compounds b1–b5 were prepared as per the process

shown in *Figure 4* using the method described below.

N-(2-(1H-indol-3-yl) ethyl)-2-chloroacetamide (9)

Chloroacetyl chloride (0.68 g, 0.48 mL, 6.0 mmol) followed by triethylamine (1.39 mL, 10 mmol) were slowly added to a stirred solution of tryptamine (0.80 g, 5.0 mmol) in dry THF (15 mL) at 0 ℃. The reaction mixture was stirred at RT for 6 h, and was then quenched by the addition of water. The mixture was diluted with EtOAc, and washed with water and brine. The organic layer was separated and dried over MgSO4, filtered and concentrated under reduced pressure to afford the title compound (1.14 g, 96%) as a white solid, which was used in the next step without further purification.

N-(2-(1H-indol-3-yl) ethyl)-2-(quinolin-8-ylamino) acetamide (b1)

Diisopropylethylamine (0.70 mL, 4.0 mmol) and NaI (0.36 g, 2.4 mmol) were added to a mixture of N-(2-(1H-indol-3-yl)ethyl)-2-chloroacetamide (0.47 g, 2.0 mmol) and 8-amino-quinoline (0.29 g, 2.0 mmol) in DMF (6 mL). The reaction mixture was heated to 80 ℃ for 8 h, and then cooled and quenched with water. The mixture was diluted with EtOAc, and washed with water and brine. The organic layer was separated and dried over MgSO4, filtered and concentrated. The resulting residue was purified by flash silica-gel column chromatography to afford the title compound (0.43 g, 63%) as a white solid. Mp 182–185 ℃. 1H NMR (400 MHz, CDCl3) δ 8.72 (dd, J=4.2, 1.6 Hz,

Page 8 of 19

Chen et al. Multifunctional agents for Alzheimer's disease

1H), 8.12 (dd, J=8.3, 1.6 Hz, 1H), 7.65 (brs, 1H), 7.49 (d, J=7.9 Hz, 1H), 7.43 (dd, J=8.3, 4.2 Hz, 1H), 7.33 (t, J=7.9 Hz, 1H), 7.24 (d, J=8.3 Hz, 1H), 7.18 (d, J=7.6 Hz, 1H), 7.12 (t, J=7.2 Hz, 1H), 7.00 (t, J=7.2 Hz, 1H), 6.85 (brs, 1H), 6.61 (d, J=2.2 Hz, 1H), 6.58 (d, J=7.2 Hz, 1H), 6.55 (brs, 1 H), 3.98 (d, J = 6.0 Hz, 2H), 3.61 (q, J=6.6 Hz, 2H), 2.90 (t, J=6.8 Hz, 2H). 13C NMR (100 MHz, CDCl3) δ 170.2, 147.4, 143.8, 138.2, 136.2, 136.1, 128.4, 127.6, 127.1, 122.0, 121.9, 121.7, 119.4, 118.6, 116.0, 112.6, 111.1, 106.0, 48.6, 39.2, and 25.3. HRMS ESI (+) m/z calculated for C21H20N4ONa [M+Na] + 367.1535, found 367.1528.

2-chloro-N-(2-(5-methoxy-1H-indol-3-yl) ethyl) acetamide (10)

Chloroacetyl chloride (0.41 g, 0.29 mL, 3.6 mmol) followed by triethylamine (0.83 mL, 6.0 mmol) were slowly added to a stirred solution of 5-methoxytryptamine (0.57 g, 3.0 mmol) in dry THF (10 mL) at 0 ℃. The reaction mixture was stirred at RT for 6 h, and then quenched by the addition of water. The mixture was diluted with EtOAc, and washed with water and brine. The organic layer was separated and dried over MgSO4, filtered and concentrated, under reduced pressure to afford the title compound (0.74 g, 93%) as a white solid, which was used in the next step without further purification.

N-(2-(5-methoxy-1H-indol-3-yl) ethyl)-2-(quinolin-8-ylamino) acetamide (b2)

Diisopropylethylamine (0.70 mL, 4.0 mmol) and NaI (0.36 g, 2.4 mmol) were added to a mixture of 2-chloro-N-(2-(5-methoxy-1H-indol-3-yl)ethyl)acetamide (0.53 g, 2.0 mmol) and 8-amino-quinoline (0.29 g, 2.0 mmol) in DMF (6 mL). The reaction mixture was heated to 80 ℃ for 8 h, and then cooled, and quenched with water. The mixture was diluted with EtOAc, and washed with water and brine. The organic layer was separated and dried over MgSO4, filtered and concentrated. The resulting residue was purified by flash silica-gel column chromatography to afford the title compound (0.57 g, 76%) as a pale-yellow solid. Mp 158–161 ℃. 1H NMR (400 MHz, CDCl3) δ 8.72 (dd, J=4.2, 1.7 Hz, 1H), 8.10 (dd, J=8.3, 1.7 Hz, 1H), 7.79 (brs, 1H), 7.41 (dd, J=8.3, 4.2 Hz, 1H), 7.31 (t, J=7.9 Hz, 1H), 7.16 (dd, J=8.2, 0.9 Hz, 1H), 7.13 (d, J=8.8 Hz, 1H), 6.95 (d, J=2.4 Hz, 1H), 6.87 (brs, 1H), 6.79 (dd, J=8.8, 2.4 Hz, 1H), 6.62–6.53 (m, 3H), 3.96 (d, J=6.0 Hz, 2H), 3.80 (s, 3H), 3.58 (q, J=6.8 Hz, 2H), 2.85 (t, J=6.9 Hz, 2H). 13C NMR (100 MHz, CDCl3) δ 170.4, 153.9, 147.4, 143.8, 138.1, 136.1, 131.4, 128.4, 127.6, 127.5, 122.8, 121.7, 116.1, 112.3, 112.2, 111.9, 106.1, 100.3, 55.9, 48.6, 39.1, and

25.4. HRMS ESI (+) m/z calculated for C22H22N4O2Na [M+Na] + 397.1640, found 397.1635.

### N-(2-(5-hydroxy-1H-indol-3-yl) ethyl)-2-(quinolin-8-ylamino) acetamide (b3)

BBr3 (3 M in CH2Cl2, 2 mL) was added to a solution of N-(2-(5-methoxy-1H-indol-3-yl) ethyl)-2-(quinolin-8-ylamino) acetamide (0.75 g, 2.0 mmol) in dry CH2Cl2 (10 mL) in an ice-water bath. The mixture was stirred overnight and quenched with aqueous NaHCO3. The mixture was extracted with THF/EA (1:2, 20 mL ×2). The combined organic layer was washed with brine and dried over MgSO4. The organic solvent was evaporated, and the residue was purified by flash silica-gel column chromatography to afford the title compound (0.51 g, 71%) as a white solid. Mp 121–124 ℃. 1H NMR (400 MHz, DMSO) δ 10.46 (s, 1H), 8.78 (dd, J=4.1, 1.6 Hz, 1H), 8.58 (s, 1H), 8.23 (dd, J=8.3, 1.5 Hz, 1H), 8.16 (t, J=5.7 Hz, 1H), 7.52 (dd, J=8.3, 4.2 Hz, 1H), 7.37 (t, J=7.9 Hz, 1H), 7.11 (dd, J=8.4, 3.8 Hz, 2H), 7.01 (d, J=2.1 Hz, 1H), 6.93 (t, J=5.5 Hz, 1H), 6.84 (d, J=2.1 Hz, 1H), 6.58 (dd, J=8.6, 2.3 Hz, 1H), 6.50 (d, J = 7.6 Hz, 1H), 3.88 (d, J=5.5 Hz, 2H), 3.37 (dd, J=14.0, 6.7 Hz, 2H), 2.74 (t, J=7.5 Hz, 2H). 13C NMR (100 MHz, DMSO) δ 169.7, 150.6, 147.6, 144.6, 138.0, 136.4, 131.3, 128.7, 128.3, 128.2, 123.6, 122.3, 114.4, 112.1, 111.7, 111.2, 105.2, 102.7, 46.8, 39.9, and 25.84. HRMS ESI (+) m/z calculated for C21H20N4O2Na [M+Na] + 383.1484, found 383.1479.

3-(2-(2-(quinolin-8-ylamino) acetamido) ethyl)-1H-indol-5-yl dimethylcarbamate (b4)

Dimethylcarbamoyl chloride (151 mg, 129 µL, 1.4 mmol) followed by diisopropylethylamine (0.35 mL, 2.0 mmol) were added to a solution of N-(2-(5-hydroxy-1H-indol-3-yl) ethyl)-2-(quinolin-8-ylamino) acetamide (0.36 g, 1.0 mmol) in dry pyridine (5 mL) at RT. The reaction mixture was heated to 70 ℃ and stirred overnight, and then cooled, and the pyridine was removed under reduced pressure. The residue was taken up in CH2Cl2 and washed with water. The organic layer was separated and dried with MgSO4, filtered and concentrated. The resulting residue was purified by flash silica-gel column chromatography to afford the title compound (0.32 g, 75%) as a white solid. Mp 97–100 ℃. 1H NMR (400 MHz, CDCl3) δ 8.70 (dd, J=4.2, 1.7 Hz, 1H), 8.20 (s, 1H), 8.07 (dd, J=8.3, 1.6 Hz, 1H), 7.38 (dd, J=8.3, 4.2 Hz, 1H), 7.32 (t, J=7.9 Hz, 1H), 7.20 (d, J=2.2 Hz, 1H), 7.16–7.12 (m, 1H), 7.09 (d, J=8.7 Hz, 1H), 6.83 (dt, J=9.1, 4.5 Hz, 2H), 6.64 (t, J=5.9 Hz, 1H), 6.57–6.53 (m, 1H), 6.51 (d, J=2.2 Hz, 1H), 3.93 (d, J=5.9 Hz, 2H), 3.47 (q, J=6.7 Hz, 2H), 3.10 (s, 3H), 3.00 (s, 3H), 2.76 (t, J=6.9 Hz, 2H). 13C NMR
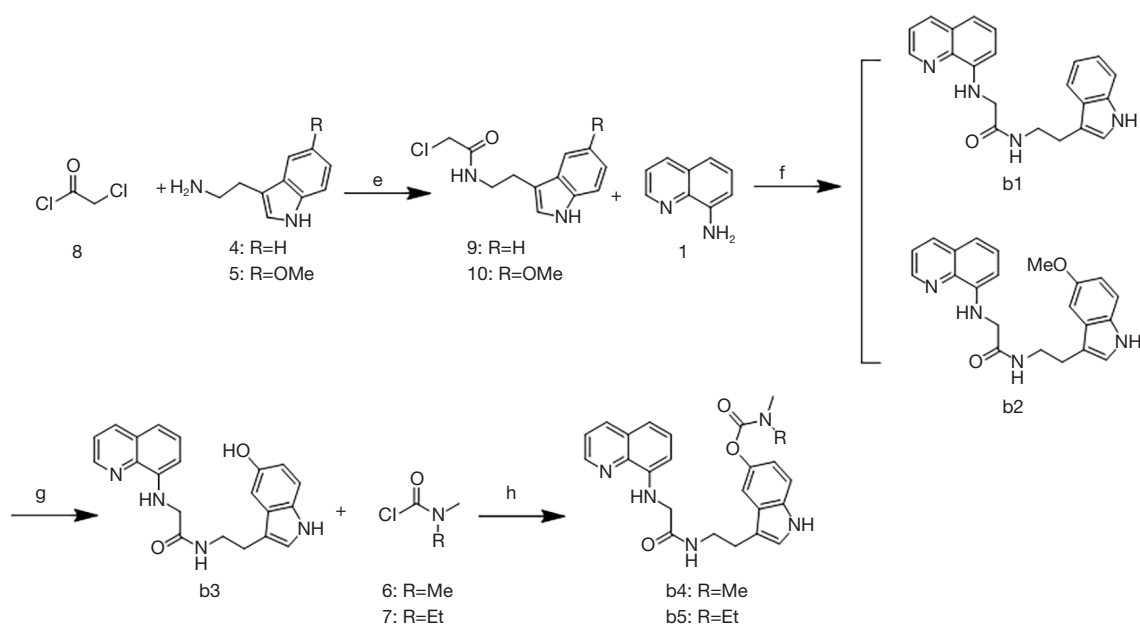
Figure 5 Synthesis of target compounds b1–b5. (e) Et₃N, THF, rt (f) NaI, i-Pr2NEt, DMF, 80 ℃, (g) BBr₃, CH₂Cl₂, ice-bath; (h) i-Pr₂NEt, pyridine, 70 ℃.

(100 MHz, CDCl3) δ 170.4, 156.1, 147.4, 144.8, 143.9, 138.2, 136.1, 133.9, 128.5, 127.6, 127.4, 123.4, 121.7, 116.4, 115.9, 112.5, 111.4, 110.9, 106.0, 48.5, 39.3, 36.7, 36.5, and 25.3. HRMS ESI (+) m/z calculated for $C_{24}H_{26}N_5O_3$ [M+H] + 432.2036, found 432.2032.

3-(2-(2-(quinolin-8-ylamino) acetamido) ethyl)-1H-indol-5-yl ethyl (methyl) carbamate (b5)

N-ethyl-N-methylcarbamoyl chloride (136 mg, 1.12 mmol) followed by diisopropylethylamine (0.28 mL, 1.6 mmol) were added to a solution of N-(2-(5-hydroxy-1H-indol-3-yl)ethyl)-2-(quinolin-8-ylamino) acetamide (0.29 g, 0.8 mmol) in dry pyridine (4.0 mL) at RT. The reaction mixture was heated to 70 ℃ and stirred overnight, and then cooled, and the pyridine was removed under reduced pressure. The residue was taken up in CH2Cl2 and washed with water. The organic layer was separated and dried with MgSO4, filtered and concentrated. The resulting residue was purified by flash silica-gel column chromatography to afford the title compound (0.26 g, 72%) as a white solid. Mp 87–90 ℃. 1H NMR (400 MHz, CDCl3) δ 8.71 (dd, J=4.2, 1.7 Hz, 1H), 8.10 (dd, J=8.3, 1.7 Hz, 1H), 7.91 (s, 1H), 7.40 (dd, J=8.3, 4.2 Hz, 1H), 7.33 (t, J=7.9 Hz, 1H), 7.21 (brs, 1H), 7.15 (dd, J=13.0, 4.8 Hz, 2H), 6.86 (d, J=8.6 Hz, 1H), 6.81 (t, J=5.8 Hz, 1H), 6.63 (t, J=5.9 Hz, 1H), 6.56 (dd, J=5.9, 1.6 Hz, 2H), 3.96 (d, J=6.0 Hz, 2H), 3.57–3.36 (m, 4H), 3.08 (s, 1.5H), 3.0 (s, 1.5H) 2.80 (t, J=6.8 Hz, 2H), 1.25 (t,

J=6.5 Hz, 1.5H), 1.18 (t, J=6.5 Hz, 1.5H). 13C NMR (100 MHz, CDCl3) δ 170.4, 155.8, 147.4, 144.8, 143.9, 138.2, 136.1, 133.9, 128.5, 127.7, 127.4, 123.4, 121.7, 116.4, 115.9, 112.5, 111.4, 110.9, 106.0, 48.5, 44.0, 39.3, 34.3, 33.8, 25.3, 13.3, and 12.6. HRMS ESI (+) m/z calculated for $C_{25}H_{28}N_5O_3$ [M+H] + 446.2192, found 446.2187.

Preparation of N-(2-(1H-indol-3-yl) ethyl) quinolin-8-amine derivatives c1–c5

The compounds c1–c5 were prepared as per the process shown in *Figure 5* using the methods described below.

3-(2-bromoethyl)-1H-indole (13)

Ph3P (3.4 g, 13 mmol) followed by CBr4 (4.64 g, 14 mmol) were added to a solution of 3-indoleethanol (1.61 g, 10.0 mmol) in MeCN (20 mL). The reaction mixture was stirred at RT for about 3 h, and then diluted with ethylacetate (20 mL), and washed with water (20 mL). The organic layer was separated, and the aqueous phase was extracted with ethylacetate (20 mL). The combined organic layers were washed with water and brine, dried over MgSO4, filtrated and concentrated. The resulting residue was purified by flash silica-gel column chromatography to afford the title compound (2.02 g, 90%) as a white solid.

N-(2-(1H-indol-3-yl) ethyl) quinolin-8-amine (c1)

K2CO3 (0.83 g, 6.0 mmol) was added to a mixture of 3-(2-bromoethyl)-1H-indole (0.67 g, 3.0 mmol) and

Page 10 of 19

Chen et al. Multifunctional agents for Alzheimer's disease

8-amino-quinoline (0.43 g, 3.0 mmol) in acetone (10 mL), and the reaction mixture was heated to reflux for 10 h, and then cooled to RT and quenched with water. The mixture was diluted with EtOAc, and washed with water and brine. The organic layer was separated and dried over MgSO4, filtered and concentrated. The resulting residue was purified by flash silica-gel column chromatography to afford the title compound (0.69 g, 80%) as a pale-yellow solid. Mp 107–110 ℃. 1H NMR (400 MHz, CDCl3) δ 8.68 (dd, J=4.2, 1.6 Hz, 1H), 8.04 (dd, J=8.3, 1.5 Hz, 1H), 8.03 (s, 1H), 7.66 (d, J=7.8 Hz, 1H), 7.38 (t, J=7.9 Hz, 1H), 7.34 (dd, J=7.6, 5.2 Hz, 2H), 7.20 (t, J=7.2 Hz, 1H), 7.13 (t, J=7.4 Hz, 1H), 7.05 (dd, J=12.0, 5.0 Hz, 2H), 6.73 (d, J=7.6 Hz, 1H), 6.29 (brs, 1H), 3.66 (t, J=7.2 Hz, 2H), 3.23 (t, J=7.2 Hz, 2H). 13C NMR (100 MHz, CDCl3) δ 146.8, 144.8, 138.3, 136.4, 136.0, 128.7, 127.9, 127.5, 122.1, 122.0, 121.4, 119.4, 118.8, 113.8, 113.7, 111.2, 104.7, 43.7, and 25.2. HRMS ESI (+) m/z calculated for C19H18N3 [M+H] + 288.1501, found 288.1494.

3-(2-bromoethyl)-5-methoxy-1H-indole (14)

Ph3P (1.02 g, 3.9 mmol) followed by CBr4 (1.39 g, 14 mmol) were added to a solution of 2-(5-methoxy-1H-indol-3-yl) ethanol (0.57 g, 3.0 mmol) in MeCN (10 mL). The reaction mixture was stirred at rt for about 3 h, and then diluted with AcOEt (15 mL) and washed with water (15 mL). The organic layer was separated, and the aqueous phase was extracted with AcOEt (15 mL). The combined organic layers were washed with water and brine, dried over MgSO4, filtrated and concentrated. The resulting residue was purified by flash silica-gel column chromatography to afford the title compound (0.51 g, 67%) as a brown oil.

N-(2-(5-methoxy-1H-indol-3-yl) ethyl) quinolin-8-amine (c2)

K2CO3 (0.55 g, 4.0 mmol) was added to a mixture of 3-(2-bromoethyl)-5-methoxy-1H-indole (0.51 g, 2.0 mmol) and 8-amino-quinoline (0.29 g, 2.0 mmol) in acetone (8 mL), and the reaction mixture was heated to reflux for 10 h, and then cooled to RT and quenched with water. The mixture was diluted with EtOAc, and washed with water and brine. The organic layer was separated and dried over MgSO4, filtered and concentrated. The resulting residue was purified by flash silica-gel column chromatography to afford the title compound (0.35 g, 55%) as a pale-yellow oil. 1H NMR (400 MHz, CDCl3) δ 8.67 (dd, J=4.2, 1.7 Hz, 1H), 8.03 (dd, J=8.3, 1.6 Hz, 1H), 7.95 (brs, 1H), 7.38 (t, J=7.9 Hz, 1H), 7.33 (dd, J=8.3, 4.2 Hz, 1H), 7.22 (d, J=8.8 Hz, 1H), 7.07 (d, J=2.3 Hz, 1H), 7.06–7.01 (m, 2H), 6.85 (dd, J=8.8, 2.4 Hz, 1H), 6.73 (d, J=7.6 Hz, 1H), 6.31 (brs, 1H), 3.81 (s, 3H), 3.64 (t, J=7.1 Hz, 2H), 3.19 (t, J=7.1 Hz, 2H). 13C NMR (100 MHz, CDCl3) δ 154.0, 146.8, 144.8, 138.3, 136.0, 131.5, 128.8, 127.9, 127.8, 122.8, 121.4, 113.8, 113.5, 112.3, 111.9, 104.7, 100.6, 55.9, 43.8, 25.2. HRMS ESI (+) m/z calculated for C20H20N3O [M+H] + 318.1606, found 318.1601.

3-(2-(quinolin-8-ylamino) ethyl)-1H-indol-5-ol (c3)

BBr3 (3 M in CH2Cl2, 1.0 mL) was added to a solution of N-(2-(5-methoxy-1H-indol-3-yl) ethyl) quinolin-8-amine (0.32 g, 1.0 mmol) in dry CH2Cl2 (5 mL) in an ice-water bath. The mixture was stirred for 6 h and quenched with aqueous NaHCO3. The mixture was extracted with THF/AcOEt (1:2, 10 mL ×2). The combined organic layer was washed with brine and dried over MgSO4, filtrated and concentrated. The resulting residue was purified by flash silica-gel column chromatography to afford the title compound (0.25 g, 82%) as a yellow solid. Mp 191–194 ℃. 1H NMR (400 MHz, CD3OD) δ 8.63 (d, J=2.7 Hz, 1H), 8.11 (d, J=8.2 Hz, 1H), 7.43–7.33 (m, 2H), 7.17 (d, J=8.6 Hz, 1H), 7.10–6.95 (m, 3H), 6.78 (d, J=7.6 Hz, 1H), 6.68 (d, J=8.6 Hz, 1H), 3.59 (t, J=7.0 Hz, 2H), 3.11 (t, J=7.0 Hz, 2H). 13C NMR (100 MHz, CD3OD) δ 149.7, 146.5, 144.6, 138.1, 135.9, 131.8, 128.9, 128.1, 127.5, 123.0, 121.0, 113.6, 111.4, 111.3, 111.0, 104.9, 102.1, 43.5, 24.7. HRMS ESI (+) m/z calculated for C19H18N3O [M+H] + 304.1450, found 304.1446.

3-(2-(quinolin-8-ylamino) ethyl)-1H-indol-5-yl dimethylcarbamate (c4)

Dimethylcarbamoyl chloride (45 mg, 38 µL, 0.42 mmol), followed by diisopropylethylamine (0.11 mL, 0.6 mmol) was added to a solution of 3-(2-(quinolin-8-ylamino)ethyl)-1H-indol-5-ol (90 mg, 0.3 mmol) in dry pyridine (1.8 mL) at RT. The reaction mixture was heated to 70 ℃ and stirred overnight, and then cooled, and the pyridine was removed under reduced pressure. The residue was taken up in CH2Cl2 and washed with water. The organic layer was separated and dried with MgSO4, filtered and concentrated. The resulting residue was purified by flash silica-gel column chromatography to afford the title compound (78 mg, 70%) as yellow oil. 1H NMR (400 MHz, CDCl3) δ 8.68 (dd, J=4.2, 1.7 Hz, 1H), 8.28 (s, 1H), 8.04 (dd, J=8.3, 1.6 Hz, 1H), 7.38 (d, J=7.9 Hz, 1H), 7.35–7.31 (m, 2H), 7.21 (d, J=8.7 Hz, 1H), 7.03 (d, J=7.5 Hz, 1H), 6.95 (d, J=2.2 Hz, 1H), 6.91 (dd, J=8.7, 2.2 Hz, 1H), 6.70 (d, J=7.5 Hz, 1H), 6.24 (brs, 1H), 3.60 (dd, J=11.3, 6.7 Hz, 2H), 3.19–3.07 (m, 5H), 3.02 (s, 3H). 13C NMR (100 MHz, CDCl3) δ 156.1, 146.8, 144.9, 144.8, 138.3, 136.0, 134.1, 128.7, 127.9, 127.7, 123.3, 121.3, 116.6, 113.7, 113.6, 111.5, 111.0,
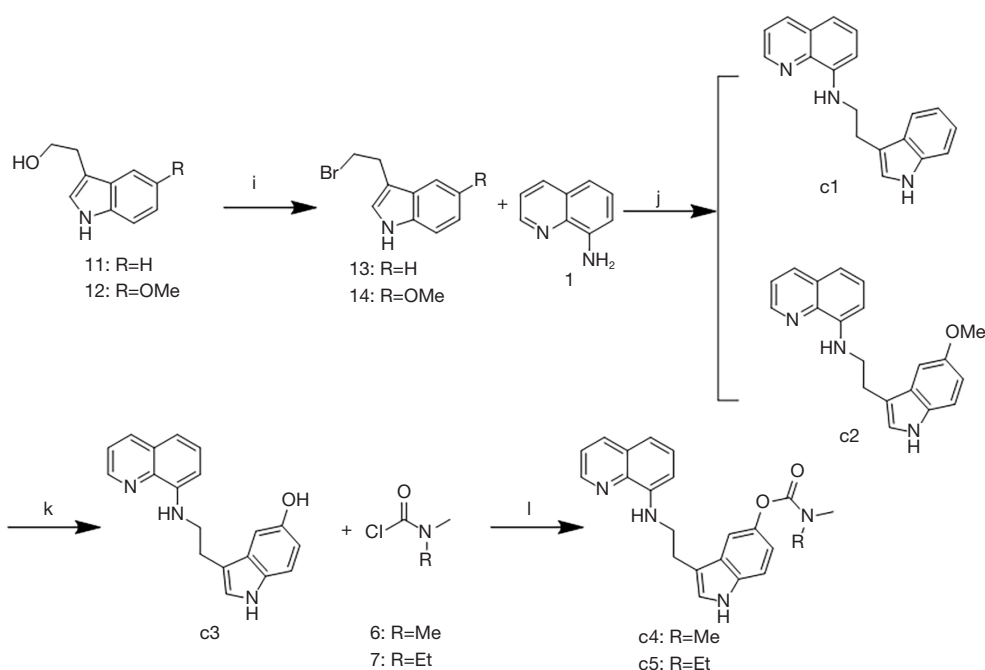
Figure 6 Synthesis of target compounds c1–c5. (i) CBr$_4$, PPh$_3$, MeCN, rt.; (j) K$_2$CO$_3$, acetone, reflux, (k) BBr$_3$, CH$_2$Cl$_2$, ice-bath; (l) i-Pr$_2$NEt, pyridine, 70 ℃.

104.8, 43.6, 36.8, 36.5, 25.1. HRMS ESI (+) m/z calculated for C22H23N4O2 [M+H] + 375.1821, found 375.1815.

3-(2-(quinolin-8-ylamino) ethyl)-1H-indol-5-yl ethyl (methyl) carbamate (c5)

N-ethyl-N-methylcarbamoyl chloride (51 mg, 0.42 mmol) followed by diisopropylethylamine (0.11 mL, 0.6 mmol) were added to a solution of 3-(2-(quinolin-8-ylamino)ethyl)-1H-indol-5-ol (90 mg, 0.3 mmol) in dry pyridine (1.8 mL) at RT. The reaction mixture was heated to 70 ℃ and stirred overnight, and then cooled, and the pyridine was removed under reduced pressure. The residue was taken up in CH2Cl2 and washed with water. The organic layer was separated and dried with MgSO4, filtered and concentrated. The resulting residue was purified by flash silica-gel column chromatography to afford the title compound (79 mg, 68%) as a yellow oil. 1H NMR (400 MHz, CDCl3) δ 8.68 (dd, J=4.2, 1.6 Hz, 1H), 8.28 (s, 1H), 8.04 (dd, J=8.3, 1.6 Hz, 1H), 7.41–7.29 (m, 3H), 7.22 (d, J=8.7 Hz, 1H), 7.03 (d, J=7.8 Hz, 1H), 6.97 (d, J=2.1 Hz, 1H), 6.92 (d, J=8.5 Hz, 1H), 6.71 (d, J=7.4 Hz, 1H), 6.25 (brs, 1H), 3.61 (d, J=3.9 Hz, 2H), 3.55–3.37 (m, 2H), 3.20–3.13 (m, 2H), 3.09 (s, 1.5H), 3.01 (s, 1.5H), 1.26 (t, J=6.9 Hz, 1.5H), 1.20 (t, J=6.9 Hz, 1.5H). 13C NMR (100 MHz, CDCl3) δ 155.8, 146.8, 144.9, 144.7, 138.2, 136.0, 134.0, 128.7, 127.8, 127.7, 123.3, 121.3, 113.7, 113.6, 111.5, 111.0, 104.7, 45.1,

44.0, 43.6, 35.7, 25.1, 12.8. HRMS ESI (+) m/z calculated for C23H25N4O2 [M+H]+ 389.1978, found 389.1973.

Results

Chemistry

The synthetic routes of the 15 target compounds (a1–a5, b1–b5, and c1–c5) are described in *Figure 4-6*. In this study, 8-aminoquinoline and the melatonin derivatives are linked through the urea group, acetyl group, and alkyl group to form a1–a5, b1–b5, and c1–c5, respectively.

The general procedure for the synthesis of the target compounds a1–a5 is presented in *Figure 4*. Compound 3 was prepared by the amidation of compound 1 and (trichloroethoxy) chloroformate 2 in the presence of i-Pr$_2$NEt. The condensation of 3 with tryptamine (4) or 5-methoxytryptamine (5) and DBU resulted in compounds a1 and a2, respectively. The demethylation of a2 resulted in compound a3. Finally, the appropriate dialkylaminocarbamoyl chloride 6 and 7 was used as the alkylating agent in the reaction of nucleophilic substitution with compound a3, and produced the products a4 or a5.

The general procedure for the synthesis of the target compounds b1–b5 is reported in *Figure 5*. Compound 8 was

Page 12 of 19

Chen et al. Multifunctional agents for Alzheimer's disease

Table 1 Inhibition of the self-induced and AChE-induced Aβ(1–40) aggregation of derivatives a1–a5, b1–b5, and c1–c5

Compounds	Inhibition of Aβ aggregation (%) ± SEM	
	Self-induced[b]	AChE-induced[c]
a1	NA	3.21±0.5
a2	NA	2.68±0.8
a3	14.1±0.7	22.03±2.7
a4	5.6±0.5	12.23±0.6
a5	NA	1.68±0.3
b1	NA	1.31±0.5
b2	1.3±0.7	3.05±2.3
b3	19.7±4.2	31.10±1.5
b4	10.1±1.5	14.35±2.5
b5	9.0±2.1	13.74
c1	0.7±0.4	2.21±0.5
c2	8.9±1.3	11.07±2.3
c3	41.4±2.1	58.17±1.8
c4	3.6±0.2	3.54±0.3
c5	25.5±3.2	35.05±2.3
Congo Red	86.5±1.4	94.3±3.5
Melatonin	NA	NA
Donepezil	ND	ND
Rivastigmine	ND	ND

[b], Inhibition of self-mediated Aβ(1–40) aggregation. The thioflavin-T fluorescence method was used, and the measurements were carried out in the presence of 10 μM inhibitor. [c], Inhibition of AChE-induced Aβ(1–40) aggregation. The thioflavin-T fluorescence method was used, and the concentration of the tested inhibitor and Aβ(1–40) was 100 μM and 230 μM, respectively, whereas the Aβ(1–40):AChE ratio was equal to 100:1. SEM, standard error of the mean; NA, not available; ND, not determined.

used as the alkylating agent in the reaction of nucleophilic substitution with compounds 4 and 5 and led to the formation of compounds 9 and 10. Compounds b1–b2 were obtained by the amination of compound 1 with compounds 9 and 10 in the presence of i-Pr$_2$NEt and NaI. The demethylation of b2 resulted in compound b3, which was then alkylated with carbamoylchloride 6 or 7 to produce b4 and b5, respectively.

Compounds c1–c5 were synthesized as described in *Figure 6*. The Appel reaction of tryptophol 11 or 5-methoxy-tryptophol 12 with CBr4 produced compounds

13 and 14, respectively. The compounds c1 and c2 were synthesized via the nucleophilic substitution reaction of compound 1 with compounds 13 and 14, respectively. The demethylation of c2 resulted in compound c3. Finally, a reaction of O-alkylation of compound c3 with compounds 6 and 7 produced compounds c4 and c5, respectively.

The structures of the target compounds were validated using ^{1}H NMR, ^{13}C NMR, and HRMS, and their purities were determined to be above 95% using HPLC.

Biological evaluation

Inhibition of Aβ aggregation
To detect the inhibitory potency of derivatives on Aβ aggregation, the thioflavin-T fluorescence assay was used with congo red, and melatonin as the reference compounds. As *Table 1* shows, compounds c3 and c5 exhibited superior inhibitory activity of self-induced Aβ(1–40) aggregation (with inhibitory rates of 41.4%±2.1% and 25.5%±3.2% at 10 μM, respectively) compared to that of other compounds. Globally, the new compounds had higher inhibitory rates than melatonin on Aβ aggregation.

Inhibition of AChE and BuChE activity
Cholinesterase is currently the most effective drug target for the treatment of AD. Melatonin had no inhibitory effect on either AChE or BuChE, and most compounds had better AChE inhibitory effects than melatonin. Additionally, the compounds for which rivastigmine pharmacophore was introduced had better AChE and BuChE inhibitory effects than the corresponding compounds. The compounds a4, a5, b4, b5, c4, and c5 had excellent BuChE inhibitory effects, and better selectivity for BuChE than AChE (see *Table 2*).

Cytotoxicity
MTT assays were performed to evaluate the cytotoxicity of our compounds to C17.2 cells. The results indicated that most of the derivatives exhibited low cytotoxicity at the concentration of 50 μM, while some compounds were still tolerable for cells up to 100 μM (see *Figure 7*). Notably, compound c1 had different effects on the cells at different concentrations; for example, the proliferation of C17.2 cells was promoted at a concentration of 50 μM, but cytotoxicity was inducted at a concentration of at 100 μM.

Protective effects against glutamate-induced HT22 cell death
Series c (i.e., compounds c1–c5) with the linker of an

Table 2 The inhibition of the AChE and BuChE activities of derivatives a1–a5, b1–b5, and c1–c5

| Compounds	IC$_{50}$ ± SEM (µM)	
	AChE[b]	BuChE[c]
a1	NA	10.3±0.7
a2	29.2±1.2	NA
a3	36.3±0.7	8.78±0.3
a4	35.6±0.6	3.3±0.2
a5	NA	2.6±0.4
b1	11.20±0.4	NA
b2	13.05±0.2	NA
b3	4.34 ±0.1	NA
b4	11.20±0.3	0.9±0.1
b5	13.74±0.6	0.8±0.1
c1	32.71±1.4	13.5±0.4
c2	NA	4.5±0.3
c3	NA	4.3±0.4
c4	NA	0.9±0.1
c5	25.05±1.7	1.1±0.1
Donepezil	0.8±0.1	ND
Melatonin	NA	NA
Rivastigmine	ND	12.8±1.2

[b], AChE from electric eel; IC50, inhibitor concentration (means ± SEM of 3 experiments) for the 50% inactivation of AChE. [c], BuChE from horse serum; IC50, inhibitor concentration (means ± SEM of 3 experiments) for the 50% inactivation of BuChE. SEM, standard error of the mean; NA, not available; ND, not determined.

alkyl group showed a promising protective effect. All 3 compounds (i.e., a3, b3, and c3) with hydroxyl-indole moiety had strong protective effects. Notably, compound c3 exhibited a significant protective effect at the low concentration of 3 µM (see *Figure 8*).

Metal-binding studies of a3 and c1

UV-Vis absorption studies of our derivatives with common divalent metal ions (e.g., Cu, Zn, magnesium, calcium, manganese, cobalt, and nickel ions) were also conducted. The results showed that the studied compounds (a3 and c1) selectively chelated the Cu ions, but had no effect on the other divalent metal ions (see *Figures 9,10*).
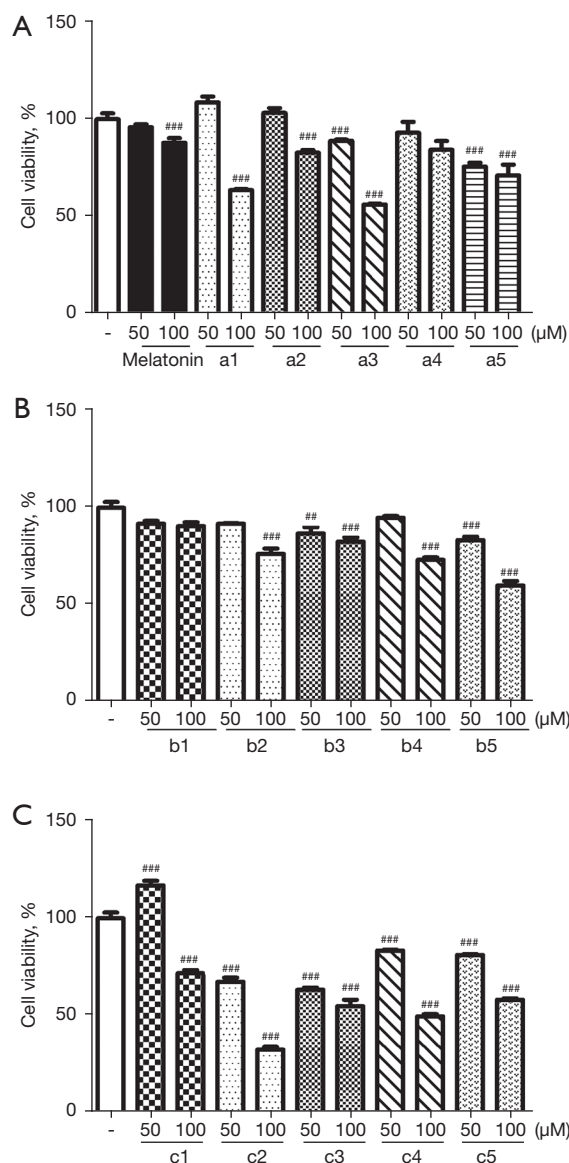
Figure 7 The cell toxicity on C17.2 cells. The C17.2 cells were treated with 50- or 100-µM test compounds for 24 h, and MTT assays were used to test cell viability. The data are presented as the mean ± SEM (n=6. ##P<0.05, ###P<0.01 *vs.* the vehicle-treated control). MTT assays, methyl thiazolyl tetrazolium assays.

Discussion

AD is an age-related neurodegenerative disease with multiple predisposing factors and complicated pathogenesis. The prevalence of AD has increased in the current rapidly aging society and contributes to a heavy burden on families and society. Despite the profound impact of AD, current

Page 14 of 19

Chen et al. Multifunctional agents for Alzheimer's disease
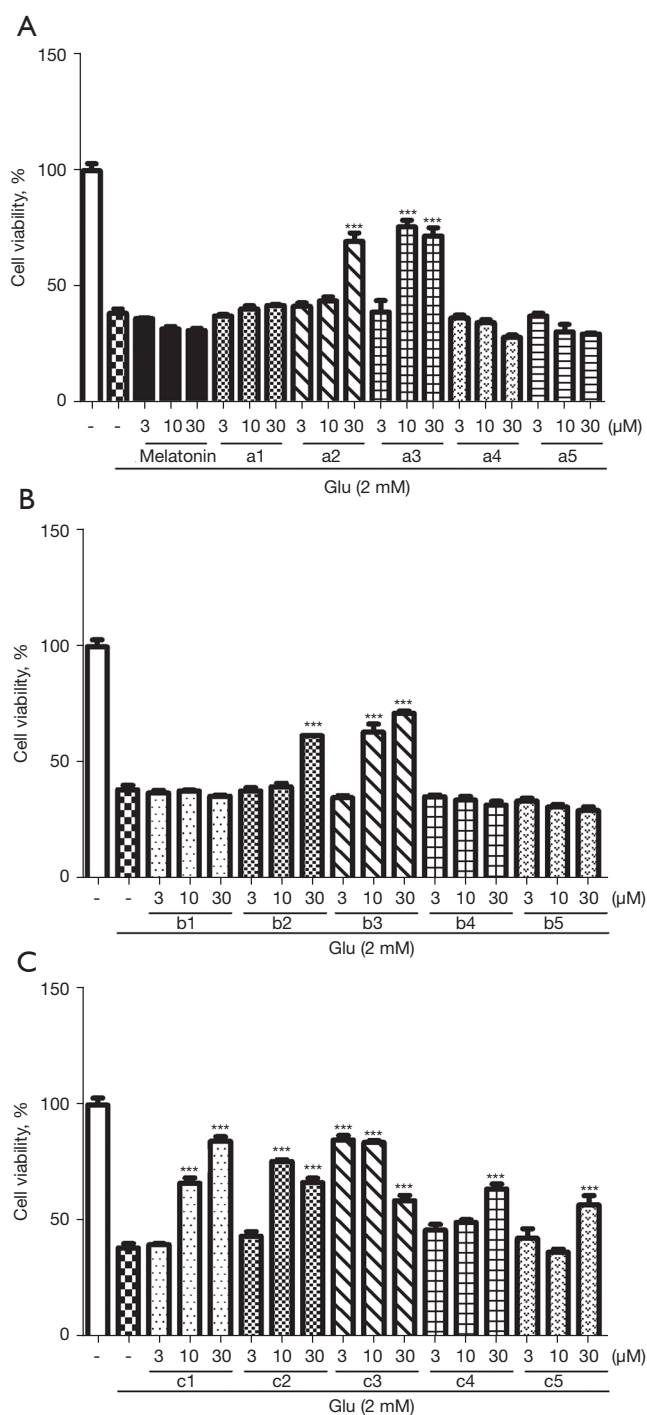
Figure 8 The neuroprotective effects of compounds against cell injury induced by glutamate in HT22 cells. The HT22 cells were treated with compounds at the indicated concentrations for 24 h with glutamate. The data are presented as the mean ± SEM (n=6. ***P<0.01). SEM, standard error of the mean.

treatments only stabilize some symptoms of early to mid-stage forms of AD for a limited period. The complex interconnection of the molecular events underpinning AD is thought to be one of the reasons for the failure of single-target-directed drug clinical trials. Thus, multi-target-directed ligands are considered an effective way to treat neurodegenerative diseases.

In this study, we designed, synthesized and evaluated 8-aminoquinoline-melatonin derivatives (i.e., a1–a5, b1–b5, and c1–c5) as effective multifunctional agents for AD. As mentioned above, amyloid aggregation is a critical step in the formation of $A\beta$ neurotoxic species and their deposition in the brain, which lead to neuroinflammation, neurite degeneration, and neuronal death, which in turn causes cognitive decline. Previous studies have shown that PBT-2 effectively reduces $A\beta_{42}$ levels in the cerebrospinal fluid of AD animals (12,31,32). To detect the inhibitory potency of derivatives on $A\beta$ aggregation, the thioflavin-T fluorescence assay was used with Congo Red and melatonin as the reference compounds. As *Table 1* shows, the inhibitory rates of the new compounds on $A\beta$ aggregation were higher than the inhibitory rate of melatonin, which was completely inactive in the same assay. This result led us to speculate that 8-aminoquinoline plays an important role in the inhibition of $A\beta$ aggregation. The linker appears to affect the $A\beta$-aggregation inhibitory activity. Compounds of series c, in which the linker is an alkyl group, showed a good effect. In particular compounds c3 and c5 showed the highest percentage of inhibition of all the compounds tested. Additionally, the type of the side chain at 5-position of the indole ring significantly affected the $A\beta$ aggregation inhibitory activity. As *Table 1* shows, the introduction of hydroxyl at 5-position of the indole ring had a better effect on the $A\beta$ aggregation inhibition, such as a3, b3, and c3, than other compounds of the same type.

Recent studies of AD patients have indicated that while AChE activity is greatly reduced in specific regions of the brain, BuChE activity is increased (33-35). Due to the involvement of BuChE in the hydrolysis of ACh, it appears that the inhibition of both types of cholinesterase enzymes is essential for the successful treatment of AD. AChE and BuChE enzyme inhibitory activity was detected. As *Table 2* shows, all the compounds had better AChE inhibitory effects than melatonin. The compounds a4, a5, b4, b5, c4, and c5 had excellent BuChE inhibitory effects and good selectivity for BuChE over AChE. Additionally, the
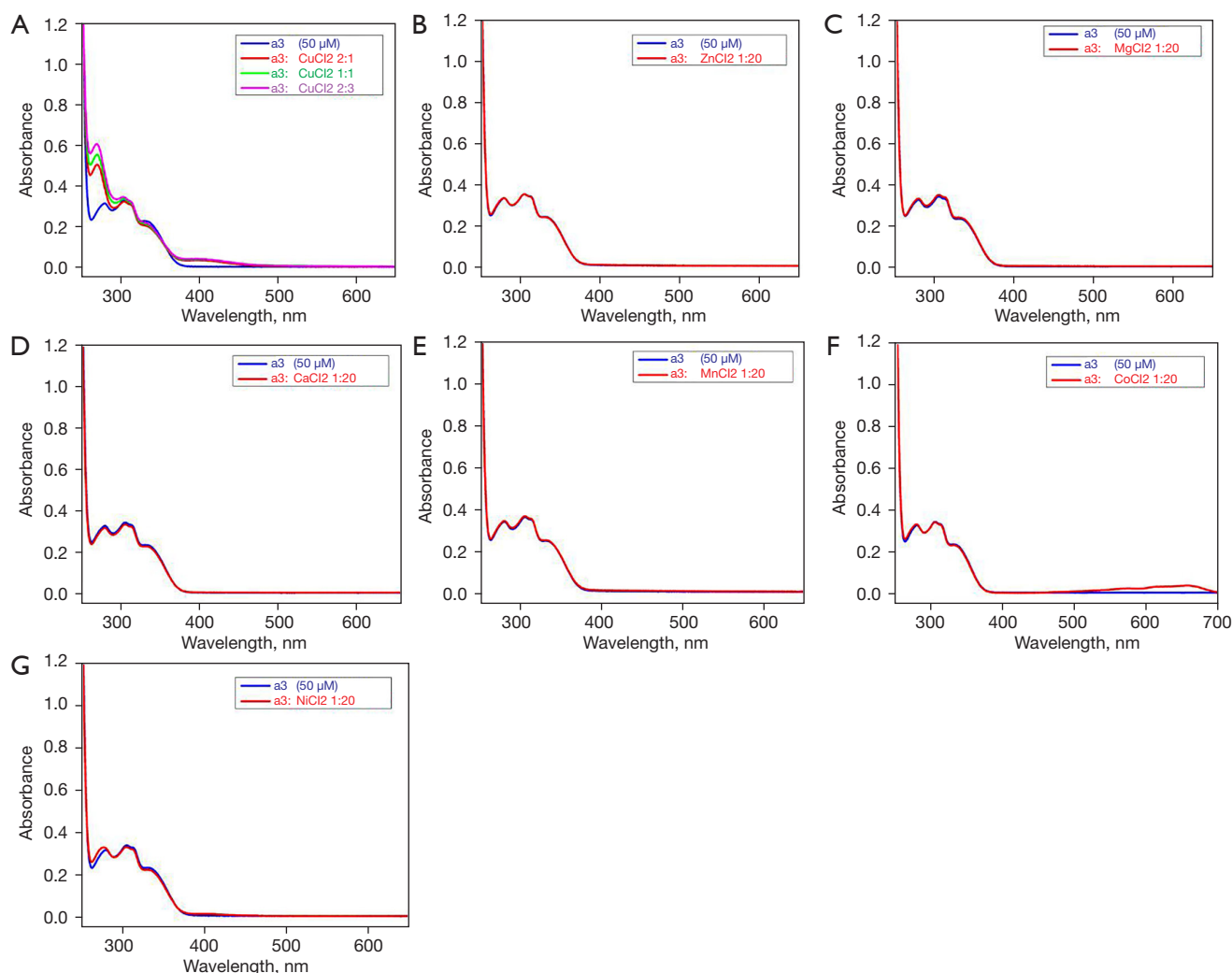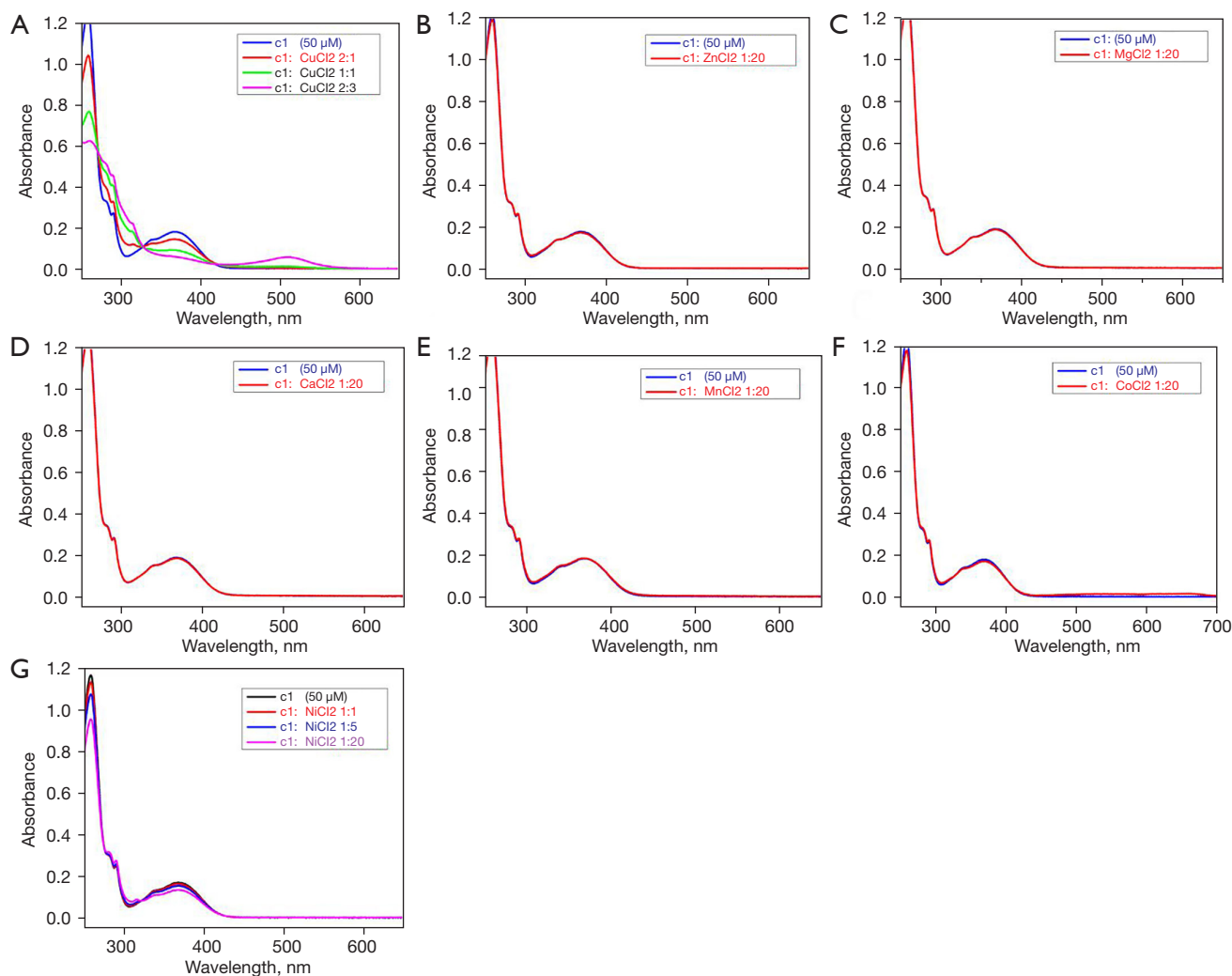
Figure 9 Ultraviolet-visible spectra of a3 (50 μM) in the presence of 1equiv (50 μM) of CuCl₂ (10-min incubation) or 20 equiv (1.0 mM) of the other biological relevant metal ions (ZnCl₂, MgCl₂, CaCl₂, MnCl₂ CoCl₂, and NiCl₂, 30-min incubation). Experimental conditions: EtOH; room temperature.

compounds for which rivastigmine pharmacophore was introduced had better AChE and BuChE inhibitory effects than the corresponding compounds.

The loss of neuronal cells is a pathological and clinical characteristic of AD. Glutamate toxicity is a common model for investigating OS-induced neuronal cell death (36). The HT22 cell line is a mouse immortalized hippocampal neuronal cell line that lacks functional glutamate receptors. Thus, it is frequently used in analyses of OS-induced neuronal cell death by exposure to high concentrations of glutamate. To determine whether our compounds protected the neuronal cells against glutamate-induced toxicity. HT22 cells were pretreated with indicated concentrations

of compounds (3–30 μM) for 30 min, and then exposed to 2 mM of glutamate for 24 h. The MTT results showed that some of the compounds still maintained the protective effect of melatonin on neuronal cells with the introduction of the 8-aminoquinoline structure (see *Figure 8*). Notably, series c (c1–c5) with the linker of an alkyl group produced a promising protective effect. All 3 compounds (i.e., a3, b3, and c3) with hydroxyl-indole moiety exhibited strong protective effects, which indicates that the hydroxyl group is very important in this activity.

Cu is essential for some of the enzymes that have a role in brain metabolism. Sophisticated mechanisms balance Cu import and export to ensure proper nutrient levels

Page 16 of 19

Chen et al. Multifunctional agents for Alzheimer's disease

Figure 10 Ultraviolet-visible spectra of c1 (50 μM) in the presence of 5equiv (0.25 mM) of $CuCl_2$ (10-min incubation) or 20 equiv (1.0 mM) of other biological relevant metal ions ($ZnCl_2$, $MgCl_2$, $CaCl_2$, $MnCl_2$ $CoCl_2$, and $NiCl_2$, 30 min incubation). Experimental conditions: EtOH; room temperature.

(homeostasis), while minimizing toxic effects. Many studies have provided information concerning the high serum levels of non-bound-to-ceruloplasmin (non-Cp-Cu), which result in reduced cognitive function, a rate of mild cognitive impairment, and AD (37-39). AD cortical tissue has an increased propensity to bind exchangeable Cu^{2+} with increasing oxidative damage and neuropathological alterations, which have been observed in AD cases. Accordingly, Cu-ion chelators were considered a promising tool for the treatment of AD. In our study, we chose a3 and c1 for a further metal-binding study. The results showed that a3 and c1 selectively chelated the Cu ions, but

had no effect on the other divalent metal ions. Thus, our compounds exhibited excellent selectivity for Cu ions over other metal ions.

Conclusions

In summary, multi-target molecules via a multi-functional drug have been widely used in the search for an effective treatment of AD. Among the synthesized compounds, c3 and c5 had superior inhibitory activity against self-induced Aβ aggregation (with inhibitory rates of 41.4±2.1 and 25.5±3.2 at 10 μM, respectively) compared to that of

other compounds. Compounds in the carbamate group showed significant BuChE inhibitory activity and excellent selectivity compared to AChE. The MTT assay results indicated that our compounds had low cytotoxicity in C17.2 cells. Most of our compounds had good protective effects on neuronal cells in relation to glutamate-induced toxicity. Additionally, compounds a3 and c1 specifically chelated with Cu ions. Taking all these promising results together, 8-aminoquinoline-melatonin hybrids can serve as lead molecules for the further development of anti-AD drugs. The further optimization of these compounds is in progress in our laboratory.

Acknowledgments

Footnote

Reporting Checklist: The authors have completed the MDAR reporting checklist. Available at https://atm.amegroups.com/article/view/10.21037/atm-22-730/rc

Data Sharing Statement: Available at https://atm.amegroups.com/article/view/10.21037/atm-22-730/dss

Conflicts of Interest: All authors have completed the ICMJE uniform disclosure form (available at https://atm.amegroups.com/article/view/10.21037/atm-22-730/coif). The authors have no conflicts of interest to declare.

Ethical Statement: The authors are accountable for all aspects of the work in ensuring that questions related to the accuracy or integrity of any part of the work are appropriately investigated and resolved.

Open Access Statement: This is an Open Access article distributed in accordance with the Creative Commons Attribution-NonCommercial-NoDerivs 4.0 International License (CC BY-NC-ND 4.0), which permits the non-commercial replication and distribution of the article with the strict proviso that no changes or edits are made and the original work is properly cited (including links to both the formal publication through the relevant DOI and the license). See: https://creativecommons.org/licenses/by-nc-nd/4.0/.

References

1. Ubhi K, Masliah E. Alzheimer's disease: recent advances and future perspectives. J Alzheimers Dis 2013;33 Suppl 1:S185-94.
2. Prince M, Bryce R, Albanese E, et al. The global prevalence of dementia: a systematic review and metaanalysis. Alzheimers Dement 2013;9:63-75.e2.
3. Bachurin SO, Bovina EV, Ustyugov AA. Drugs in Clinical Trials for Alzheimer's Disease: The Major Trends. Med Res Rev 2017;37:1186-225.
4. Hardy J, Selkoe DJ. The amyloid hypothesis of Alzheimer's disease: progress and problems on the road to therapeutics. Science 2002;297:353-6.
5. Mohamed T, Shakeri A, Rao PP. Amyloid cascade in Alzheimer's disease: Recent advances in medicinal chemistry. Eur J Med Chem 2016;113:258-72.
6. Mullane K, Williams M. Alzheimer's therapeutics: continued clinical failures question the validity of the amyloid hypothesis-but what lies beyond? Biochem Pharmacol 2013;85:289-305.
7. Jakob-Roetne R, Jacobsen H. Alzheimer's disease: from pathology to therapeutic approaches. Angew Chem Int Ed Engl 2009;48:3030-59.
8. Nesi G, Sestito S, Digiacomo M, et al. Oxidative Stress, Mitochondrial Abnormalities and Proteins Deposition: Multitarget Approaches in Alzheimer's Disease. Curr Top Med Chem 2017;17:3062-79.
9. Chen WT, Liao YH, Yu HM, et al. Distinct effects of $Zn2+$, $Cu2+$, $Fe3+$, and $Al3+$ on amyloid-beta stability, oligomerization, and aggregation: amyloid-beta destabilization promotes annular protofibril formation. J Biol Chem 2011;286:9646-56.
10. Liu G, Huang W, Moir RD, et al. Metal exposure and Alzheimer's pathogenesis. J Struct Biol 2006;155:45-51.
11. Zatta P, Lucchini R, van Rensburg SJ, et al. The role of metals in neurodegenerative processes: aluminum, manganese, and zinc. Brain Res Bull 2003;62:15-28.
12. Adlard PA, Cherny RA, Finkelstein DI, et al. Rapid restoration of cognition in Alzheimer's transgenic mice with 8-hydroxy quinoline analogs is associated with decreased interstitial Abeta. Neuron 2008;59:43-55.

Page 18 of 19

Chen et al. Multifunctional agents for Alzheimer's disease

13. Grossi C, Francese S, Casini A, et al. Clioquinol decreases amyloid-beta burden and reduces working memory impairment in a transgenic mouse model of Alzheimer's disease. J Alzheimers Dis 2009;17:423-40.

14. Oliveri V, Vecchio G. 8-Hydroxyquinolines in medicinal chemistry: A structural perspective. Eur J Med Chem 2016;120:252-74.

15. Faux NG, Ritchie CW, Gunn A, et al. PBT2 rapidly improves cognition in Alzheimer's Disease: additional phase II analyses. J Alzheimers Dis 2010;20:509-16.

16. Crouch PJ, Savva MS, Hung LW, et al. The Alzheimer's therapeutic PBT2 promotes amyloid-beta degradation and GSK3 phosphorylation via a metal chaperone activity. J Neurochem 2011;119:220-30.

17. Wang L, Esteban G, Ojima M, et al. Donepezil + propargylamine + 8-hydroxyquinoline hybrids as new multifunctional metal-chelators, ChE and MAO inhibitors for the potential treatment of Alzheimer's disease. Eur J Med Chem 2014;80:543-61.

18. Deraeve C, Boldron C, Maraval A, et al. Preparation and study of new poly-8-hydroxyquinoline chelators for an anti-Alzheimer strategy. Chemistry 2008;14:682-96.

19. Tahmasebinia F, Emadi S. Effect of metal chelators on the aggregation of beta-amyloid peptides in the presence of copper and iron. Biometals 2017;30:285-93.

20. Sarell CJ, Syme CD, Rigby SE, et al. Copper(II) binding to amyloid-beta fibrils of Alzheimer's disease reveals a picomolar affinity: stoichiometry and coordination geometry are independent of Abeta oligomeric form. Biochemistry 2009;48:4388-402.

21. Hossain MF, Uddin MS, Uddin GMS, et al. Melatonin in Alzheimer's Disease: A Latent Endogenous Regulator of Neurogenesis to Mitigate Alzheimer's Neuropathology. Mol Neurobiol 2019;56:8255-76.

22. Alghamdi BS. The neuroprotective role of melatonin in neurological disorders. J Neurosci Res 2018;96:1136-49.

23. Chen C, Yang C, Wang J, et al. Melatonin ameliorates cognitive deficits through improving mitophagy in a mouse model of Alzheimer's disease. J Pineal Res 2021;71:e12774.

24. Wu YH, Feenstra MG, Zhou JN, et al. Molecular changes underlying reduced pineal melatonin levels in Alzheimer disease: alterations in preclinical and clinical stages. J Clin Endocrinol Metab 2003;88:5898-906.

25. Wu YH, Swaab DF. The human pineal gland and melatonin in aging and Alzheimer's disease. J Pineal Res 2005;38:145-52.

26. Hampel H, Mesulam MM, Cuello AC, et al. The cholinergic system in the pathophysiology and treatment of Alzheimer's disease. Brain 2018;141:1917-33.

27. Kandiah N, Pai MC, Senanarong V, et al. Rivastigmine: the advantages of dual inhibition of acetylcholinesterase and butyrylcholinesterase and its role in subcortical vascular dementia and Parkinson's disease dementia. Clin Interv Aging 2017;12:697-707.

28. Liu S, Dang M, Lei Y, et al. Ajmalicine and its Analogues Against AChE and BuChE for the Management of Alzheimer's Disease: An In-silico Study. Curr Pharm Des 2020;26:4808-14.

29. Zhou S, Huang G. The biological activities of butyrylcholinesterase inhibitors. Biomed Pharmacother 2022;146:112556.

30. Bartorelli L, Giraldi C, Saccardo M, et al. Effects of switching from an AChE inhibitor to a dual AChE-BuChE inhibitor in patients with Alzheimer's disease. Curr Med Res Opin 2005;21:1809-18.

31. Bharti K, Majeed AB, Prakash A. Possible role of metal ionophore against zinc induced cognitive dysfunction in D-galactose senescent mice. Biometals 2016;29:399-409.

32. Adlard PA, Parncutt J, Lal V, et al. Metal chaperones prevent zinc-mediated cognitive decline. Neurobiol Dis 2015;81:196-202.

33. Mushtaq G, Greig NH, Khan JA, et al. Status of acetylcholinesterase and butyrylcholinesterase in Alzheimer's disease and type 2 diabetes mellitus. CNS Neurol Disord Drug Targets 2014;13:1432-9.

34. Greig NH, Lahiri DK, Sambamurti K. Butyrylcholinesterase: an important new target in Alzheimer's disease therapy. Int Psychogeriatr 2002;14 Suppl 1:77-91.

35. Perry EK, Perry RH, Blessed G, et al. Changes in brain cholinesterases in senile dementia of Alzheimer type. Neuropathol Appl Neurobiol 1978;4:273-7.

36. Lewerenz J, Maher P. Chronic Glutamate Toxicity in Neurodegenerative Diseases-What is the Evidence? Front Neurosci 2015;9:469.

37. Squitti R, Barbati G, Rossi L, et al. Excess of nonceruloplasmin serum copper in AD correlates with MMSE, CSF beta-amyloid, and h-tau. Neurology 2006;67:76-82.

38. Squitti R, Simonelli I, Ventriglia M, et al. Meta-analysis of serum non-ceruloplasmin copper in Alzheimer's disease. J

Alzheimers Dis 2014;38:809-22.

39. Squitti R, Ghidoni R, Simonelli I, et al. Copper dyshomeostasis in Wilson disease and Alzheimer's disease as shown by serum and urine copper indicators. J Trace Elem Med Biol 2018;45:181-8.

(English Language Editor: L. Huleatt)